University of Groningen

Strain-Modulated Charge Transport in Flexible PbS Nanocrystal Field-Effect Transistors

Nugraha, Mohamad Insan; Matsui, Hiroyuki; Watanabe, Shun; Kubo, Takayoshi; Hausermann, Roger; Bisri, Satria Zulkarnaen; Sytnyk, Mykhailo; Heiss, Wolfgang; Loi, Maria Antonietta; Takeya, Jun

IMPORTANT NOTE: You are advised to consult the publisher's version (publisher's PDF) if you wish to cite from it. Please check the document version below.

Document Version
Publisher's PDF, also known as Version of record

[Link to publication in University of Groningen/UMCG research database](#)

COMMUNICATION

Strain-Modulated Charge Transport in Flexible PbS Nanocrystal Field-Effect Transistors

Mohamad Insan Nugraha, Hiroyuki Matsui, Shun Watanabe, Takayoshi Kubo, Roger Häusermann, Satria Zulkarnaen Bisri, Mykhailo Sytnyk, Wolfgang Heiss, Maria Antonietta Loi,* and Jun Takeya*

Extensive progresses in understanding charge carrier transport in semiconducting colloidal nanocrystals (NCs) have provided hope to exploit this class of materials for low-temperature processed electronic and optoelectronic devices. Among many types of NCs, lead chalcogenide (PbX; X = S, Se, Te) systems are the most promising because they have large Bohr exciton radius leading to strong quantum confinement, thus high absorbance, and at the same time they allow easy synthetic control of size and shape.[1–6] In solution, these NCs are coated with long-alkyl chain ligands, which maintain their structural properties as well as give them solubility in most organic solvents. Once deposited into solid films, these long ligands need to be replaced with shorter ones to strengthen electronic coupling as well as allow tunneling of charge carriers between nanocrystals, thus improving film conductivity. Importantly, this ligand exchange can be easily done either in solution phase or in solid phase, both techniques are compatible with solution

M. I. Nugraha, Prof. H. Matsui, Dr. S. Watanabe,
T. Kubo, Dr. R. Häusermann, Prof. J. Takeya
Department of Advanced Materials Science
Graduate School of Frontier Sciences
The University of Tokyo
5-1-5 Kashiwanoha, Kashiwa, Chiba 277-8561, Japan
E-mail: takeya@k.u-tokyo.ac.jp
M. I. Nugraha, Prof. M. A. Loi
Zernike Institute for Advanced Materials
University of Groningen
Nijenborgh 4, Groningen 9747AG, The Netherlands
E-mail: m.a.loi@rug.nl
Prof. H. Matsui
Research Center for Organic Electronics
Yamagata University
4-3-16 Jonan, Yonezawa, Yamagata 992-8510, Japan
Prof. S. Watanabe
JST
PRESTO
4-1-8 Honcho, Kawaguchi, Saitama 332-0012, Japan
Dr. S. Z. Bisri
RIKEN Center for Emergent Matter Science (CEMS)
2-1 Hirosawa, Wako, Saitama 351-0198, Japan
Dr. M. Sytnyk, Prof. W. Heiss
Materials for Electronics and Energy Technology (i-MEET)
Friedrich-Alexander-Universität
Erlangen-Nürnberg
Martensstraße 7, 91058 Erlangen, Germany
Dr. M. Sytnyk, Prof. W. Heiss
Energie Campus Nürnberg (EnCN)
Fürther Straße 250, 90429 Nürnberg, Germany

processable fabrication methods such as spin-coating, dip-coating, ink-jet printing, etc.[7–12] This solution processability, combined with low temperature processing, opens up opportunities to use this material to fabricate electronic and optoelectronic devices on flexible plastic substrates.[13,14]

As the active materials are deposited onto flexible substrates, bending, folding, or stretching of the substrate is able to induce mechanical strain on the active layer which influences the characteristics of the fabricated devices. Recently, mechanical strain effects have been intensively investigated on organic semiconductor thin film transistors (TFTs).[15–17] The application of compressive strain on pentacene films has allowed improving the film conductivity and carrier mobility in TFT devices as a consequence of reduced molecular spacing. Oppositely, applied strain produces increased spacing which leads to the decrease in the carrier mobility.[16–19] The effect of mechanical strain on lead chalcogenide NC devices, particularly in TFTs, is still poorly investigated. As the bulk moduli of organic ligands has been reported to be lower than the NC cores, the introduction of mechanical strain is expected to have a great impact on the properties of the fabricated devices, with the potential to improve charge mobility in this system.[1,20] Therefore, the effect of mechanical strain on the electrical properties of NC-TFTs needs to be addressed to further understand their physical properties as well as to strengthen the applicability of NCs for diverse applications.

Here, we report a study of the effect of mechanical strain on the electrical characteristics of PbS field-effect transistors (FETs). As a gate dielectric, we use ion gel, which is able to accumulate high carrier concentration leading to electron mobility as high as 2.1 cm^2 V^{-1} s^{-1}. Upon the application of compressive strain, we observe improvement in the source–drain current, which leads to an increase in the electron mobility up to 45% at 2% strain. This improvement is associated to the reduced barrier length between NCs due to the bending of the crosslinking ligands. In the opposite strain direction, we observe reduction in the electron mobility which is an indication of the increase of the NC distance. Interestingly, we find that the change in the electron mobility is followed by the variation in the threshold voltages of the devices depending on the direction of the strain. The decreased threshold voltages as the compressive strain is applied can be attributed to the increase of the transfer integral between the NC arrays, which results in a more efficient trap filling, thus reducing carrier trapping. Meanwhile, the increased carrier traps can be responsible for the increase of the threshold voltages with the application of tensile strain. Furthermore, the observed larger effect during the application of

**ADVANCED
ELECTRONIC
MATERIALS**
www.advelectronicmat.de

**ADVANCED
SCIENCE NEWS**
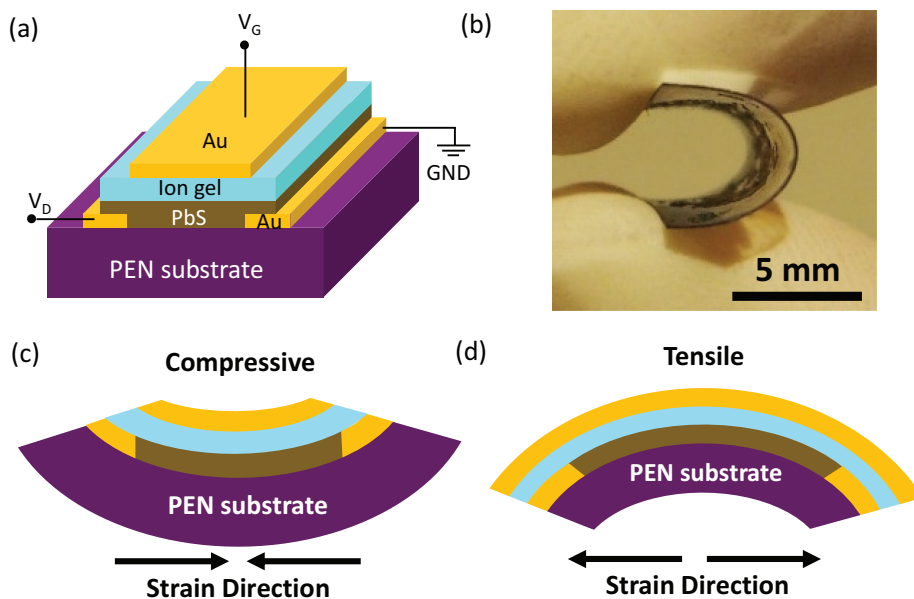www.advancedsciencenews.com

COMMUNICATION

Figure 1. a) Device structure, b) photograph of PbS NC-FETs on flexible substrate, and schematic of c) compressive (bent downward) and d) tensile strain (bent upward) applied on the devices.

tensile strain than that with compressive strain can be associated to the increase of the barrier potential due to the activation of one or more ligand chains.

To perform strain effect measurement on the PbS films, we fabricated FETs using polyethylene naphthalate (PEN) as a substrate. As source–drain electrodes, we used bottom contact Au with Cr as adhesive layer. The deposition of PbS films on the PEN substrate was performed using spin-casting similarly as previously reported.[7,21] To improve the conductivity of the semiconducting films, the long oleic acid ligands surrounding the NC surfaces were replaced with short molecules, 1,2-ethan-edithiol (EDT). Both PbS film deposition and the ligand exchange process were done using sequential layer-by-layer spin-coating procedure to ensure complete removal of the long ligands. As gate dielectric, we utilized an ion gel derived from mixing the ionic liquid 1-hexyl-3-methyl-imidazolium bis(trifluoromethanesulfonyl)imide (HMIM-TFSI) with the gelling polymer, poly(vinylidene fluoride-hexafluoropropylene) (PVDF-HFP). This mixture allows us obtaining a solid gate dielectric which is easy to handle and suitable for electronic devices fabricated on plastic substrate. In this work, the ion gel is used to accumulate high carrier concentration at the dielectric/semi-conductor interface, which can fill the carrier traps in the NCs. In the past, our group has demonstrated ion gel-gated PbS NC-FETs with electron mobility higher than 2 cm^2 V^{-1} s^{-1}.[22,23] As a gate electrode, a thin layer of Au was deposited on the top of the ion gel film. The final configuration of the fabricated devices is shown in **Figure 1**a. All the fabrication and measurements were performed in a nitrogen-filled glove box.

The flexibility of the fabricated devices is displayed in the photograph reported in Figure 1b. With this flexibility, we are able to apply compressive and tensile strain on the devices, continuously up to 2% without breaking the devices. The schematic of how the compressive and tensile strain is applied is

shown in Figure 1c. To estimate the strain (ε) applied on the devices, we first calculate the radius of curvature (R) using the following formula[24,25]

$$R = \frac{l}{2\pi\sqrt{\dfrac{dl}{l} - \dfrac{\pi^2 h^2}{12l^2}}} \tag{1}$$

where h, l, and dl are the total thickness, the initial length, and the change of length of the samples, respectively. The strain can be simply estimated from $\varepsilon = (h/2R)100\%$.[24,25] The photographs of the samples during the strain measurements are shown in Figure S1 of the Supporting Information. At first we performed surface morphology characterization of the PbS films after the application of the mechanical strain. The atomic force microscopy (AFM) images shown in Figures S2 and S3 of the Supporting Information confirm that no cracks are observed after applying compressive and tensile strain up to 2%. The transfer characteristics of the devices in the pristine condition (without strain) are shown in **Figure 2**a. The devices show a small hysteresis (<1.3 V) in the transfer curves, indicating that the ion gel provides good protection for the devices against bias stress and an effective filling of the traps.[26] Importantly, the devices show clear current modulation with very low operation voltage (<2 V), which is promising for future low energy consuming solution processable electronic devices. In the negative gate voltage, we observed a weak hole current, since the hole current is much lower than the electron current and quite close to the level of the gate leakage current; we only investigated the strain effect on the electron transport.

The threshold voltage of the devices is as low as 0.9 V. The capacitance of the ion gel (C_i) is 2.7 µF cm^{-2} at 10 Hz, allowing the very low operation voltage. The sweeping speed used for the FET measurements was 100 mV s^{-1}. The electron mobility
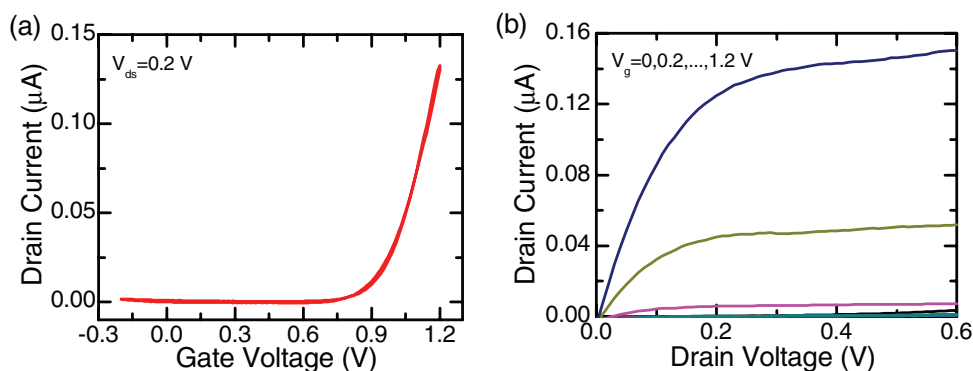
**ADVANCED
SCIENCE NEWS**
www.advancedsciencenews.com

**ADVANCED
ELECTRONIC
MATERIALS**
www.advelectronicmat.de

COMMUNICATION

Figure 2. a) I_D–V_G transfer characteristics and b) I_D–V_D output characteristics of PbS NC-FETs with HMIM-TFSI ion gel on PEN substrate.

(μ) was extracted from the linear regime, using the following equation

$$\mu = \frac{L}{WC_i V_{ds}} \frac{\partial I_{ds}}{\partial V_g} \qquad (2)$$

where V_{ds}, W, and L are source–drain voltage, channel width, and channel length. The channel length of the devices was designed to be 150 µm to minimize the effect of contact resistance. Moreover, a channel width of 70 µm was used to avoid localized surface morphology defects formed during film deposition as well as during ligand exchange, which may obscure the effect of the mechanical strain. Using Equation (2), we extracted linear electron mobility as high as 2.1 cm² V⁻¹ s⁻¹. To our knowledge, this is the highest mobility value reported in PbS NC-FETs on flexible substrate (**Table 1**). In addition, the output characteristics shown in Figure 2b indicate that the devices do not show any contact limitation at low drain voltage. Moreover, the clear saturation profiles confirm that the fabricated FETs are well performing.

Figure 3a presents the transfer characteristics of the devices under several static compressive strains. We applied compressive strain starting from 0.75% up to 2% with the interval of 0.25%. Upon the application of compressive strain, we observed an improvement in the on-current of the devices. This improvement is also followed by the shifting of the transfer curve toward more negative voltages, i.e., showing a

reduced threshold voltage as displayed in Figure S5 of the Supporting Information. Importantly, the variation of the transfer curve upon the application of compressive strain is reversible, demonstrating that the devices are still elastic after the strain is applied and that the current increase is not caused by its drifting. When the opposite strain direction (tensile strain) is applied on the devices, we observed the decrease of the on-current. The transfer characteristics measured after the application of the tensile strain are displayed in Figure 3b. In addition, we also observed the shift of the transfer curve toward more positive voltages, thus an increased threshold voltage. To have a confirmation that the variation of the on-current is not caused by changes in the dielectric properties of the gate, the gate leakage I_G–V_G characteristics of the devices under several applied mechanical strain were measured (Figure S6, Supporting Information). The measurements confirm the absence of significant changes in the gate leakage characteristics indicating that the

Table 1. Reported electron mobility in PbS FETs. (3-mercaptopropionic acid (3MPA), 1,2-ethanedithiol (EDT), ammoniumthiocyanate (NH₄SCN), tetrabuthylammoniumiodide (TBAI), methylammoniumiodide (MAI)).

Substrates	Dielectrics	Ligands/treatment	Maximum mobility [cm² V⁻¹ s⁻¹]
Si/SiO₂	SiO₂	3MPA, EDT, NH₄SCN, TBAI, MAI	0.07[7,8,21,27]
Si/SiO₂	Cytop	3MPA	0.2[7]
Kapton	Parylene	NH₄SCN	0.2[5]
Polyimide	Al₂O₃	NH₄SCN	0.47[28]
Si/SiO₂	Al₂O₃/SiO₂	Na₂S/PbCl₂	0.5[29]
Si/SiO₂	PVDF-trFE-CFE	EDT	1.1[30]
Si/SiO₂	EMIM-TFSI ion gel	3MPA	2[22]

Figure 3. I_D–V_G transfer characteristics with the application of a) compressive and b) tensile strain.

ADVANCED
ELECTRONIC
MATERIALS
www.advelectronicmat.de

ADVANCED
SCIENCE NEWS
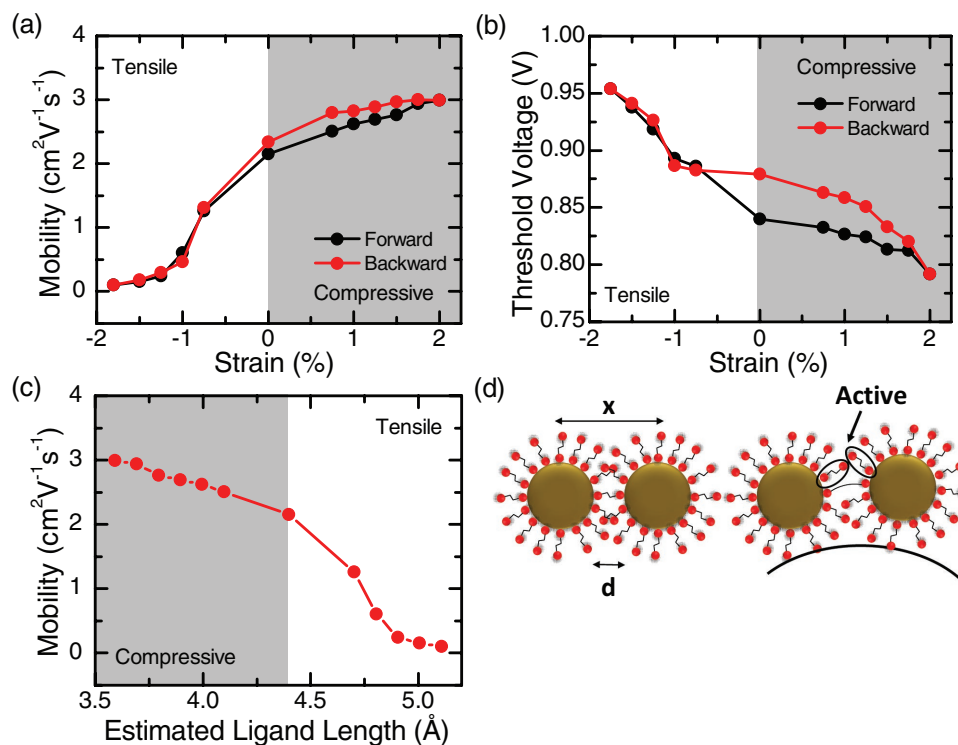www.advancedsciencenews.com

COMMUNICATION

Figure 4. a) Electron mobility, b) threshold voltage of the devices, c) relationship between electron mobility and estimated ligand length as compressive and tensile strain are applied. d) Unbound (active) ligand chains during the application of tensile strain.

carrier density, thus the capacitance of the ion gel, is not influenced by the application of the strain.

To have better description about the influence of the mechanical strain on the electrical characteristics of the devices we extracted the electron mobility for each strain condition. **Figure 4**a shows the electron mobility versus strain. Under compressive strain, the electron mobility increases with increasing strain. We attributed these results to the reduced barrier length, thus the reduction of the NC-interspacing. At 2% strain (R = 3.1 mm), we observed an improvement in the electron mobility up to 45%. Therefore with this strain, we further achieved the highest electron mobility reported in PbS NC-FETs on flexible plastic substrate. Similar to the current–voltage characteristics, the variation of mobility is reversible in the range of the applied strain, which confirms that the devices are still elastic. Under mechanical strain up to 2%, no cracks are observed on the PbS films as shown in Figures S2–S4 of the Supporting information. However, we start observing cracks on the sample after applying higher strain (see Supporting Information, Figure S4). Meanwhile, with the application of tensile strain, we observed the decrease of the electron mobility. These results can be associated to the increase of the barrier length (longer NC-interspacing) when the tensile strain is applied as displayed in Figure 4a. The variation of the NC-interspacing by applying external pressure was reported in PbS colloidal quantum dots.[1,20] In this system, uniaxial compressive pressure determines a red shift of the excitonic peak absorption. Due to higher bulk modulus of the NC cores with respect to the ligands, this shift can be mainly associated to the reduced particle spacing due to the bending of the ligands.[1,20] The

application of compressive strain on organic semiconductor FETs has also been reported to lead to improvement of carrier mobility due to reduced molecular spacing.[16,17] The introduction of tensile strain in organic FETs results in an increased molecular spacing leading to reduced charge carrier mobility.[17,19] For organic TFTs, it has also been proposed that suppressed molecular vibration can be a possible origin of the increased charge carrier mobility.[31]

Another possible origin for the increased electron mobility by applying compressive strain is the reduction of the trap density in the devices. In nanocrystal solids, the charge carrier transport mechanism is generally governed by quantum tunneling between NCs. This process strongly depends on the exchange coupling energy (β), which can be written as follows[9]

$$\beta = \hbar \exp\left\{-2\left(2m^* E_b / \hbar^2\right)^{1/2} d\right\} \tag{3}$$

where $\hbar$, m^*, and E_b are reduced Planck constant, carriers effective mass, and potential barrier height, respectively. The distance between NCs, which is proportional to the length of the ligands, is given by d. When compressive strain is applied, the bending of the crosslinking ligands leads to the reduced NC distance, thus improving the exchange coupling energy. This increased exchange coupling energy will, in turn, reduce the carrier traps near the nanocrystal band-edge as indicated in the schematics reported in Figure S7 of the Supporting Information. Conversely, the application of tensile strain will result in the reduction of the exchange coupling energy. As a consequence, some carrier traps will be introduced in the band edge of the nanocrystals. Our analysis on this trap modulation is

also supported by the observed threshold voltage shifts upon the application of the strain as shown in Figure 4b. As compressive strain increases, the threshold voltages decrease indicating a lower energy for electron accumulation, which is related to the reduction of the traps in the devices. When tensile strain is applied, we observe the increase of the threshold voltage in the devices. This threshold voltage shift explains the increase of energy for electron accumulation, which can be attributed to the increased number of carrier traps. This fluctuation of density of states due to the change of the exchange coupling bandwidth was previously observed in organic semiconductors.[32–34]

In Figure 4a,b, we report a non-fully-symmetrical profile in the variation of the device characteristics by comparing the conditions between compressive and tensile strain. At this point, the effect of tensile strain on the device characteristics is larger than that with compressive strain. This result can be explained by the induction of a potential barrier with the introduction of tensile strain. To understand this effect, we can first estimate the change of the NC-interspacing due to the applied strain (ε) using equation $\Delta x = x\varepsilon$, where x is the distance between the center of mass of the NCs as displayed in Figure 4c. When compressive strain is applied, the NC-interspacing is the only parameter changed due to the bending of the ligands. When the tensile strain is applied on the NC films, the NC-interspacing is increased by bending the crosslinking organic ligands. Due to this bending, at some points, one of thiol end groups on the NC surfaces can also become active as described in Figure 4d. These active thiols may increase the potential barrier between NCs, which results in the reduced number of the ligands interconnecting the PbS NCs, thus reducing the tunneling probability between NCs as indicated in Equation (3). In addition, the change of ligand dielectric constant when the ligands are squeezed can be another possible origin for the change of barrier potential height.

To estimate the potential barrier (E_b), we use Wentzel–Kramers–Brillouin (WKB) approximation $\beta_e = (2m*E_b/{}^2)^{1/2}$.[35] The tunneling decay constant (β_e) can be calculated from the gradient of the curve of the calculated mobility versus estimated ligand length ($d + \Delta x$). We found that β_e is a factor of 5 higher in the regime with tensile strain application ($\beta_e = 4.3$ Å^{-1}) than that with compressive strain ($\beta_e = 0.86$ Å^{-1}) indicating increased potential barrier by referring to the WKB approximation. Our explanation is in line with the previous reports showing that unbound (active) highest occupied molecular orbital (HOMO)–lowest unoccupied molecular orbital (LUMO) gap for alkane chains is as high as 8–10 eV which is about 2 eV higher than that for bound (nonactive) ligands.[35] The lower potential barrier in the ligands bound on the NC surfaces can be attributed to the hybridization of the organic ligand chains and the orbitals of the NC surface atoms, which can introduce some density of states in the molecular junction.

In conclusion, we have conducted a study of the effect of mechanical compressive and tensile strain on the electrical characteristics of PbS NC-FETs. After the application of the mechanical strain, the electron mobility is improved up to 45% at 2% compressive strain, which is attributed to the reduced NC-interspacing due to the bending of the ligands. The NC-interspacing can be increased by applying tensile strain,

which results in a reduced electron mobility. The variation of the electron mobility by applying mechanical strain is followed by a variation of the threshold voltages of the devices. With the application of compressive strain, the threshold voltages increase due to the improved transfer integral between the NC arrays and reduced carrier traps. In the opposite strain direction, carrier traps are induced by reducing the exchange coupling energy, which in turn leads to a decreased transfer integral of the NC arrays. The application of tensile strain gives rise to a larger effect than that of the compressive strain. This finding can be associated to an increase of the potential barrier due to the activation of some of the thiol ligands. Our results provide fundamental understanding of the effect of mechanical forces on PbS films which can enhance and broaden the applicability of these materials for flexible cheap solution processable electronic devices and also open new prospective toward the fabrication of mechanical force sensors.

Experimental Section

Device Fabrication: We used PEN with thickness of 125 µm as a substrate. Before use, the substrate was annealed at 150 °C for 3 h on a hot plate to remove residual monomer on the PEN surfaces. The substrate was cleaned with isopropanol for 10 min and dried with nitrogen. Cr and Au (10 nm/30 nm) were then evaporated on the clean PEN substrate as source–drain contacts.

PbS nanocrystals were synthesized following a method reported in the literature.[4] The deposition of PbS semiconducting thin film was done by spin coating 10 mg mL^{-1} of the oleic acid-capped NC solution in chloroform. To improve the film conductivity, the long-alkyl-chain oleic acid ligands were replaced by shorter organic molecules, EDT with concentration of 1% v/v in acetonitrile. The film deposition and ligand exchange (LE) were done using layer-by-layer spin coating procedures for seven times to ensure complete LE process. After each LE process, the film was cleaned with pure acetonitrile to remove old native ligands. The devices were annealed at 120 °C for 20 min to remove residual solvents and promote stronger coupling between NCs.

Ion gel based on HMIM-TFSI ionic liquid was used as gate dielectric. To synthesize the solution of ion gel, we first dissolved 80 mg of PVDF-HFP pellets in 1 mL dimethylformamide. The solution was stirred at 60 °C overnight. 20 mg of HMIM-TFSI ionic liquid was then added into the PVDF-HFP solution and stirred at room temperature for 3 h. The ion gel solution was then spin-coated on the PbS film and annealed at 90 °C for 2 h. Finally, Au with thickness of 50 nm was evaporated on the top of the ion gel film as top gate electrode. All device fabrication was performed in an N$_2$-filled glove box.

Device Measurement and Strain Effect Experiment: The FET electrical characteristics were measured by using an Agilent B1500A semiconductor parameter analyzer connected to a probe station in an N$_2$-filled glove box. For strain effect measurement, the devices were stressed using strain measurement apparatus as displayed in Figure S1 of the Supporting Information. The change of the device length was measured by using a calliper and then used in Equation (1) to further calculate the strain. The initial ligand length (without strain) was estimated using the Gaussian software. Before performing the electrical transport measurement, we wait for 10 min after changing each level of strain to relax some slow ionic migration of the ion gel.

Supporting Information

Supporting Information is available from the Wiley Online Library or from the author.

ADVANCED
ELECTRONIC
MATERIALS
www.advelectronicmat.de

ADVANCED
SCIENCE NEWS
www.advancedsciencenews.com

COMMUNICATION

Acknowledgements

[1] K. Bian, B. T. Richards, H. Yang, W. Bassett, F. W. Wise, Z. Wang, T. Hanrath, *Phys. Chem. Chem. Phys.* **2014**, *16*, 8515.

[2] L. Cademartiri, J. Bertolotti, R. Sapienza, D. S. Wiersma, G. von Freymann, G. A. Ozin, *J. Phys. Chem. B* **2006**, *110*, 671.

[3] D. N. Dirin, S. Dreyfuss, M. I. Bodnarchuk, G. Nedelcu, P. Papagiorgis, G. Itskos, M. V. Kovalenko, *J. Am. Chem. Soc.* **2014**, *136*, 6550.

[4] M. A. Hines, G. D. Scholes, *Adv. Mater.* **2003**, *15*, 1844.

[5] W. Koh, S. R. Saudari, A. T. Fafarman, C. R. Kagan, C. B. Murray, *Nano Lett.* **2011**, *11*, 4764.

[6] M. Zhao, F. Yang, C. Liang, D. Wang, D. Ding, J. Lv, J. Zhang, W. Hu, C. Lu, Z. Tang, *Adv. Funct. Mater.* **2016**, *26*, 5182.

[7] M. I. Nugraha, R. Häusermann, S. Z. Bisri, H. Matsui, M. Sytnyk, W. Heiss, J. Takeya, M. A. Loi, *Adv. Mater.* **2015**, *27*, 2107.

[8] D. M. Balazs, D. N. Dirin, H.-H. Fang, L. Protesescu, G. H. ten Brink, B. J. Kooi, M. V. Kovalenko, M. A. Loi, *ACS Nano* **2015**, *9*, 11951.

[9] D. V Talapin, J.-S. Lee, M. V Kovalenko, E. V. Shevchenko, *Chem. Rev.* **2010**, *110*, 389.

[10] M. V Kovalenko, M. Scheele, D. V Talapin, *Science* **2009**, *324*, 1417.

[11] M. V Kovalenko, M. I. Bodnarchuk, J. Zaumseil, J.-S. Lee, D. V Talapin, *J. Am. Chem. Soc.* **2010**, *132*, 10085.

[12] E. J. D. Klem, H. Shukla, S. Hinds, D. D. MacNeil, L. Levina, E. H. Sargent, *Appl. Phys. Lett.* **2008**, *92*, 212105.

[13] F. S. Stinner, Y. Lai, D. B. Straus, B. T. Diroll, D. K. Kim, C. B. Murray, C. R. Kagan, *Nano Lett.* **2015**, *15*, 7155.

[14] J.-H. Choi, H. Wang, S. J. Oh, T. Paik, P. Sung, J. Sung, X. Ye, T. Zhao, B. T. Diroll, C. B. Murray, C. R. Kagan, *Science* **2016**, *352*, 205.

[15] S. H. Nam, P. J. Jeon, S. W. Min, Y. T. Lee, E. Y. Park, S. Im, *Adv. Funct. Mater.* **2014**, *24*, 4413.

[16] P. Cosseddu, G. Tiddia, S. Milita, A. Bonfiglio, *Org. Electron.* **2013**, *14*, 206.

[17] T. Sekitani, Y. Kato, S. Iba, H. Shinaoka, T. Someya, T. Sakurai, S. Takagi, *Appl. Phys. Lett.* **2005**, *86*, 1.

[18] T. Sekine, K. Fukuda, D. Kumaki, S. Tokito, *Jpn. J. Appl. Phys.* **2015**, *54*, 04DK10.

[19] K. Fukuda, K. Hikichi, T. Sekine, Y. Takeda, T. Minamiki, D. Kumaki, S. Tokito, *Sci. Rep.* **2013**, *3*, 2048.

[20] K. Bian, A. K. Singh, R. G. Hennig, Z. Wang, T. Hanrath, *Nano Lett.* **2014**, *14*, 4763.

[21] D. M. Balazs, M. I. Nugraha, S. Z. Bisri, M. Sytnyk, W. Heiss, M. A. Loi, *Appl. Phys. Lett.* **2014**, *104*, 112104.

[22] S. Z. Bisri, C. Piliego, M. Yarema, W. Heiss, M. A. Loi, *Adv. Mater.* **2013**, *25*, 4309.

[23] S. Z. Bisri, E. Degoli, N. Spallanzani, G. Krishnan, B. J. Kooi, C. Ghica, M. Yarema, W. Heiss, O. Pulci, S. Ossicini, M. A. Loi, *Adv. Mater.* **2014**, *26*, 5639.

[24] S. Il Park, J. H. Ahn, X. Feng, S. Wang, Y. Huang, J. A. Rogers, *Adv. Funct. Mater.* **2008**, *18*, 2673.

[25] S. P. Timoshenko, J. M. Gere, *Theory of Elastic Stability*, 2nd ed, McGraw Hill, New York **1961**, Ch. 2 and 9.

[26] Y. Zhang, Q. Chen, A. P. Alivisatos, M. Salmeron, *Nano Lett.* **2015**, *15*, 4657.

[27] T. P. Osedach, N. Zhao, T. L. Andrew, P. R. Brown, D. D. Wanger, D. B. Strasfeld, L. Y. Chang, M. G. Bawendi, V. Bulović, *ACS Nano* **2012**, *6*, 3121.

[28] C. H. Jo, J. H. Kim, J. Kim, J. Kim, M. S. Oh, M. S. Kang, M. Kim, Y. Kim, B. Ju, S. K. Park, *J. Mater. Chem. C* **2014**, *2*, 10305.

[29] S. J. Oh, N. E. Berry, J.-H. Choi, E. A. Gaulding, H. Lin, T. Paik, B. T. Diroll, S. Muramoto, C. B. Murray, C. R. Kagan, *Nano Lett.* **2014**, *14*, 1559.

[30] A. G. Shulga, L. Piveteau, S. Z. Bisri, M. V. Kovalenko, M. A. Loi, *Adv. Electron. Mater.* **2016**, *2*, 1500467.

[31] T. Kubo, R. Häusermann, J. Tsurumi, J. Soeda, Y. Okada, Y. Yamashita, N. Akamatsu, A. Shishido, C. Mitsui, T. Okamoto, S. Yanagisawa, H. Matsui, J. Takeya, *Nat. Commun.* **2016**, *7*, 11156.

[32] A. Troisi, *Mol. Simul.* **2006**, *32*, 707.

[33] A. Troisi, G. Orlandi, *J. Phys. Chem. A* **2006**, *110*, 4065.

[34] A. Troisi, G. Orlandi, *Phys. Rev. Lett.* **2006**, *96*, 1.

[35] Y. Liu, M. Gibbs, J. Puthussery, S. Gaik, R. Ihly, H. W. Hillhouse, M. Law, *Nano Lett.* **2010**, *10*, 1960.